


Event-triggered H_∞ control for Takagi-Sugeno fuzzy wind turbine system

M. Syed Ali ¹, B. Vigneshwar ², S. Sanober ³, T. F. Ibrahim ⁴, F. D. Alanazi ⁵ and F. M. Osman Birkea ⁶

^{1,2} *Complex Systems and Networked Science Research Laboratory, Department of Mathematics, Thiruvalluvar University, Vellore-632115, Tamil Nadu, India*

³ *Computer Science Department, Old Dominion University Norfolk Virginia, USA.*

⁴ *Department of Mathematics, Applied faculty in Mahayel, King Khalid University, Abha, Saudi Arabia.*

⁵ *Department of Mathematics, College of Science, Northern Border University, Arar, Saudi Arabia.*

⁶ *Department of Mathematics, College of Science, Northern Border University, Arar, Saudi Arabia.*

syedjessi@gmail.com, bvigneshwar1998@gmail.com, sumayacsdept@gmail.com
tfoze@kku.edu.sa, faizah.alanazi@nbu.edu.sa, fathia.birkia@nbu.edu.sa

Abstract

In this paper, we propose an H_∞ state feedback control method for variable-speed wind turbine systems (WTSS) based on an event-triggered scheme (ETS). First, proposed the event-triggered mechanism, its threshold parameter is constructed as a special diagonal matrix which can improve system performance by flexibly adjusting the matrix elements. The main advantage of utilizing the event-triggered control is because it will activate the controllers with a user-designed event-triggering condition that helps to restrict the unnecessary network transmissions and reduce the leakages. Then, the concept of coupling leakage time-varying delay is proposed to construct a more generalized T-S fuzzy model. Subsequently, two novel integral inequalities are introduced. By the virtue of fuzzy Lyapunov function, intensive attention is focused on deriving the theoretical-based sufficient conditions in terms of solvable linear matrix inequalities (LMIs), which ensure the asymptotically stability of the closed-loop model based on Lyapunov stability theory. Then, the desirable control gains are obtained by solving the LMIs with bounds of sampling intervals. Detailed numerical simulations are performed with an experimental range of system parameters that illustrates the effectiveness of the proposed event-triggered scheme.

Keywords: Event-triggered scheme, H_∞ control, T-S fuzzy rule, wind turbine system, external disturbances.

1 Introduction

In recent decades, interest in renewable energy has surged among various research communities due to its cost-effectiveness, the rapid depletion of fossil fuels, and pollution-free nature [3, 31, 38]. Firstly, the challenge must be resolved urgently, especially for engineering critical to security, such as wind turbines [41], power grids [27] and nuclear environments [22]. The wind energy source is one of the best alternative energy sources instead of fossil fuels since it produces efficient energy with high power quality. The performance of the plant may be compromised by unanticipated abnormalities and variations, which can be irreversible. This problem can be resolved with the use of renewable energy sources, as they are not harmful to the environment. Because of its lowest price, fast growth, and guaranteed output (instead of solar, biomass and hydropower) wind energy is a major factor in addressing energy demand [4, 34]. There is considerable effort underway to improve the performance of wind turbine systems (WTSS) by improving control trajectory, tracking maximum power points and achieving stable performance [21, 23]. To an evident, authors in [18] have reviewed the technological developments of wind turbine systems under various types of advanced generators, converter topologies, proportional-integral derivative feedback controls, fuzzy-based controllers, sliding-mode controllers, adaptive controllers and many others have been proposed in the literature to stabilize nonlinear wind turbines [14, 26, 30].

Takagi-Sugeno (T-S) method is widely used in the literature for nonlinear models expressed through linear sub models using fuzzy membership-based IF-THEN rules [46]. the T-S fuzzy model was utilized for flight control systems, satellite control, and guidance systems, where it helps manage nonlinearities in dynamic flight environments [1, 8, 20]. According to [8], it can be found that the T-S fuzzy model can be used in chemical and manufacturing processes for monitoring, control, and fault diagnosis, ensuring optimal operation even in uncertain or varying environments. For example, it has been applied for trajectory tracking, adaptive control, and motion planning in robotic systems, where flexibility and precision are crucial [6, 28, 45]. These innovations are expected to extend the application of T-S fuzzy models and LMI-based control designs to emerging fields such as autonomous systems, smart grids, and advanced robotics, where the demand for robust, adaptive, and efficient control solutions continues to grow [25, 32, 42]. Moreover, a weighted ranking switching mechanism based on alterable weights is employed by the authors to stabilize discrete-time T-S fuzzy systems in real time [5]. A survey of the literature search has illustrated that the controller synthesis and filter design for T-S fuzzy wind turbine systems have attracted a lot of research efforts [16, 43].

Different types of control strategies have been proposed which provides insights into the qualitative properties of event triggered control, proportional integral derivative (PID), sliding mode control (SMC), neural networks, fuzzy-based control and predictive control [9, 10, 24, 33, 35, 39]. Even if the current measurement has barely changed from the earlier one, many useless messages may still be sent in the real world [40]. To an improvement, ETC schemes come into the picture that has an ability to utilize the communication bandwidth in an effective manner, that is, transmissions of information between the controller and wind turbine system is activated only through satisfying the pre-defined event-triggering condition rather than periodical [11]. A fuzzy control problem for inverted pendulum systems was investigated by using the event-triggered mechanism in [37]. In response to the above-mentioned discussions, this study develops a continuous-time T-S fuzzy system with event-triggered control using dynamic memories [19]. However, in order to obtain the above results, continuous sampling was required on a periodic basis [44]. Even though, the ETC scheme have been proposed for both linear and nonlinear systems, the particular industrial problem is not yet involved into the validation of control scheme [12, 15, 13].

Mathematics modeling can provide a better understanding of the dynamical characteristics of nonlinear systems by analyzing their stability and bifurcation [2]. Wind turbine stability and stabilization are analyzed using both continuous-time differential models and discrete-time differential models, see [17]. Many control methods have been proposed to deal with nonlinearity, such as output feedback control, optimal control, fuzzy control, sliding mode control, etc [29, 36]. Specifically, the Lyapunov stability theory has been used by the authors to demonstrate the stability of a hybrid wind model that includes a doubly-fed induction generator and a permanent magnet synchronous machine [47]. Furthermore, using existing mathematical methods to solve and study nonlinear models is much more complicated as the nonlinearities have changed [7].

Inspired by the aforementioned discussion, we aim to design on event-triggered control for T-S fuzzy wind turbine systems with H_∞ performance. In this regard, we have proposed the event-triggered control scheme which is considered to be an appropriate control that has an ability to handle the communication delays, packet loss and leakages. The main contributions of this paper can be summarized as follows:

- An event-triggered scheme is introduced into the network-based fuzzy controller which include the transmission delay $\tau(\mathfrak{s})$ with both lower and upper bounds, which needs to be improved only the upper bound.
- Following that, the sufficient conditions are be derived in terms of solvable LMIs through constructing the fuzzy membership-dependent Lyapunov function that helps to derive the suitable control gain matrices, which guarantee the stabilization of wind turbine systems.
- Two new integral inequalities are introduced for calculating the derivative of time-dependent LKF, which can effectively reduce the conservativeness. A less conservative stability condition is deduced by combining Wirtinger-based inequality and a refined matrix inequality.
- By taking direct wind speed as an external disturbance, some LMI-based sufficient conditions are derived to guarantee the asymptotic stability of the addressed wind turbine system and satisfy H_∞ performance index.
- Numerical simulations are performed with the parameter values, which shows the effectiveness of proposed results.

The rest of this study is organized as follows: Section 2 gives the model formulations. The H_∞ stability and stabilization criterion are derived in Section 3. The numerical results are provided in Section 4. Section 5 concludes this study.

Notation: The n -dimensional Euclidean space and its set of all $q \times p$ real matrices are denoted by the symbols \mathbb{R}^q and $\mathbb{R}^{q \times p}$, respectively. Unit and zero matrices are denoted with \mathcal{I} and 0 , respectively. Besides, $\mathbb{P} > 0 (< 0)$ indicates that the matrix \mathbb{P} is a positive (negative) definite. Additionally, symmetric terms are indicated by the mark ' $*$ '.

2 Problem formulation

In this subsection, we present the mathematical model of variable-speed wind turbine systems. As we know, a generator, wind turbine, and an electric motor drive train are the major components of wind turbine systems. The complete schematic diagram of wind turbine system is provided in Figure 1. The main aim of this study is to stabilize the nonlinear variable-speed wind turbine system and improve its dynamic performance.

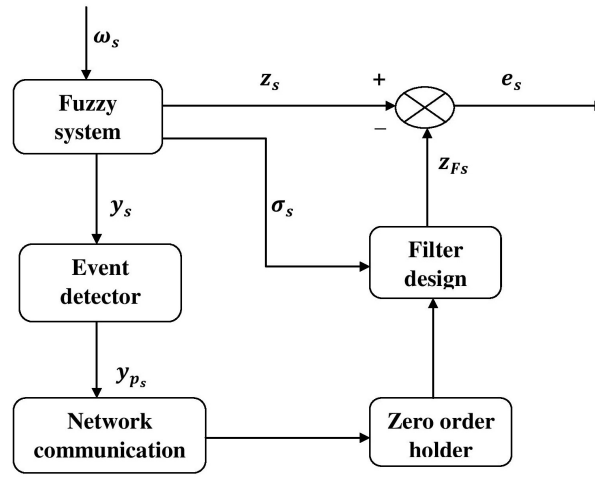


Figure 1: The mechanical model of wind turbine system

The following state-space equation describes the mathematical model of nonlinear wind turbine systems:

$$\begin{cases} \mathbf{G}_r \tilde{\Psi}_{\mathbf{R}}(\alpha(\mathfrak{s})) &= \mathbb{J}_r - \mathbf{M}_l \Psi_{\mathbf{R}}(\alpha(\mathfrak{s})) + \mathbf{M}_l \Psi_{\mathbf{g}}(\alpha(\mathfrak{s})) - \mathbf{N}_l \Phi(\alpha(\mathfrak{s})) \\ \mathbf{G}_{\mathbf{g}} \tilde{\Psi}_{\mathbf{g}}(\alpha(\mathfrak{s})) &= -\mathbb{J}_{\mathbf{g}} - \mathbf{M}_l \Psi_P(\alpha(\mathfrak{s})) + \mathbf{M}_l \Psi_{\mathbf{g}}(\alpha(\mathfrak{s})) - \mathbf{N}_l \Phi(\alpha(\mathfrak{s})) \\ \tilde{\Phi}(\alpha(\mathfrak{s})) &= \Psi_P(\alpha(\mathfrak{s})) - \Psi_{\mathbf{g}}(\alpha(\mathfrak{s})). \end{cases} \quad (1)$$

The rotational speed of the turbine, the generator's rotational speed, and the torsion angle are denoted by $\Psi_{\mathbf{R}}(\alpha(\mathfrak{s}))$, $\Psi_{\mathbf{g}}(\alpha(\mathfrak{s}))$ and respectively $\Phi(\alpha(\mathfrak{s}))$. A damping coefficient equal to \mathbf{M}_l and a stiffness coefficient equal to \mathbf{N}_l . Inertia of the rotor and generator is represented by \mathbf{G}_r and $\mathbf{G}_{\mathbf{g}}$, while aerodynamic torque and electro-magnetic torque are represented by \mathbb{J}_r and $\mathbb{J}_{\mathbf{g}}$.

Defining aerodynamic torque is as follows:

$$\mathbb{J}_r = \frac{\pi \hat{\rho} r^3 C_p(\Lambda, \eta) \mathbb{V}^2}{2\Lambda}, \quad (2)$$

$$\Lambda = \frac{r \Psi_{\mathbf{R}}(\alpha(\mathfrak{s}))}{\mathbb{V}}. \quad (3)$$

This equation represents the rotor radius, actual pitch angle, tip speed ratio, air density and aerodynamic coefficient as r , η , Λ , $\hat{\rho}$ and $C_p(\Lambda, \eta)$ respectively. In (2) proves that \mathbb{J}_r is time-varying with respect to \mathbb{V} . Linearly, aerodynamic torque is expressed as follows:

$$\mathbb{J}_r = \mathbb{J}_{r\mathbb{V}}(\varsigma)\mathbb{V}(\alpha(\mathfrak{s})) + \mathbb{J}_{r\eta}(\varsigma)\eta(\alpha(\mathfrak{s})) + \mathbb{J}_{r\Psi_{\mathbf{R}}}(\varsigma)\Psi_{\mathbf{R}}(\alpha(\mathfrak{s})), \quad (4)$$

where

$$\begin{aligned} \mathbb{J}_{r\mathbb{V}}(\varsigma) &= \frac{\partial \mathbb{J}_r}{\partial \mathbb{V}} = \pi \rho r^3 \mathbb{V} \mathcal{C}_q - \frac{\pi \rho r^3 \mathbb{V} \Lambda}{2} \frac{\partial \mathcal{C}_q}{\partial \Lambda}, \\ \mathbb{J}_{r\Psi_{\mathbf{R}}}(\varsigma) &= \frac{\partial \mathbb{J}_r}{\partial \Psi_{\mathbf{R}}} = \frac{\pi \rho r^4 \mathbb{V}}{2} \frac{\partial \mathcal{C}_q}{\partial \Lambda}, \\ \mathbb{J}_{r\eta}(\varsigma) &= \frac{\partial \mathbb{J}_r}{\partial \eta} = \frac{\pi \rho r^3 \mathbb{V}^2}{2} \frac{\partial \mathcal{C}_q}{\partial \eta}, \end{aligned}$$

with $\varsigma = [\mathbb{V}, \Psi_{\mathbf{R}}, \eta]^T$ and $\mathcal{C}_q = \frac{c_p(\Lambda, \eta)}{\Lambda}$.

Electromagnetic torque is defined as follows:

$$\mathbb{J}_{\mathbf{g}} = \mathbf{M}_g \Psi_{\mathbf{g}}(\alpha(\mathfrak{s})) - \mathbf{M}_g \mathbb{J}_{\mathbf{g}, Ref}, \quad (5)$$

The speed of zero-torque is represented by $\mathbb{J}_{\mathbf{g}, Ref}$. Specifically, $\mathbb{J}_{\mathbf{g}}$ is a nonlinear function of $\Psi_{\mathbf{g}}$ and $\mathbb{J}_{\mathbf{g}, Ref}$.

Hydraulic pitch is defined as follows:

$$\tilde{\eta}(\alpha(\mathfrak{s})) = \frac{1}{\iota}(\eta_d - \eta), \quad (6)$$

For pitch dynamics, ι represents the fixed time delay and η_d the reference pitch angle, respectively. Combining (1)-(6), we get

$$\begin{cases} \dot{x}(\alpha(\mathfrak{s})) &= \mathbf{A}(\varsigma)x(\alpha(\mathfrak{s})) + \mathbf{B}u(\alpha(\mathfrak{s})) + \mathbf{C}\mathbb{V}(\alpha(\mathfrak{s})) \\ y(\mathfrak{s}) &= \mathbf{E}x(\alpha(\mathfrak{s})) + \mathbf{D}u(\alpha(\mathfrak{s})), \end{cases} \quad (7)$$

where

$$x(\alpha(\mathfrak{s})) = [\Psi(\alpha(\mathfrak{s})) \quad \Psi_{\mathbf{R}}(\alpha(\mathfrak{s})) \quad \Psi_{\mathbf{g}}(\alpha(\mathfrak{s})) \quad \eta(\alpha(\mathfrak{s}))]^T,$$

$$u(\alpha(\mathfrak{s})) = [\eta_d \quad \mathbb{J}_{\mathbf{g}, Ref}], \quad y(\alpha(\mathfrak{s})) = [\Psi_{\mathbf{g}}(\alpha(\mathfrak{s})) \quad \mathbb{J}_{\mathbf{g}}],$$

$$\mathbf{A}(\varsigma) = \begin{bmatrix} 0 & 1 & -1 & 0 \\ -\frac{\mathbf{N}_l}{\mathbf{G}_r} & -\frac{\mathbb{J}_{r\Psi_{\mathbf{R}}}(\varsigma) + \mathbf{M}_l}{\mathbf{G}_r} & \frac{\mathbf{M}_l}{\mathbf{G}_r} & \frac{\mathbb{J}_{r\eta}(\varsigma)}{\mathbf{G}_r} \\ \frac{\mathbf{N}_l}{\mathbf{G}_g} & \frac{\mathbf{M}_l}{\mathbf{G}_g} & -\frac{\mathbf{M}_l + \mathbf{M}_g}{\mathbf{G}_g} & 0 \\ 0 & 0 & 0 & -\frac{1}{\iota} \end{bmatrix}, \quad \mathbf{B} = \begin{bmatrix} 0 & 0 \\ 0 & 0 \\ 0 & \frac{\mathbf{M}_g}{\mathbf{G}_g} \\ \frac{1}{\iota} & 0 \end{bmatrix}, \quad \mathbf{C} = \begin{bmatrix} 0 \\ \frac{\mathbb{J}_{r\mathbb{V}}(\varsigma)}{\mathbf{G}_g} \\ 0 \\ 0 \end{bmatrix},$$

$$\mathbf{E} = \begin{bmatrix} 0 & 0 & 1 & 0 \\ 0 & 0 & \mathbf{M}_l & 0 \end{bmatrix}, \quad \mathbf{D} = \begin{bmatrix} 0 & 0 \\ -\mathbf{M}_l & 0 \end{bmatrix},$$

In the wind turbine system, pitch angle operating range and wind speed range are considered as $\eta(\alpha(\mathfrak{s})) \in [\eta_m, \eta_M]^\circ$ and $\mathbb{V}(\alpha(\mathfrak{s})) \in [\mathbb{V}_m, \mathbb{V}_M]$, respectively.

2.1 T-S fuzzy modeling

Consider the following T-S fuzzy model with time-varying delays:

Plant Rule φ_1 : IF $\eta(\alpha(\mathfrak{s}))$ is \mathfrak{F}_i , and $\mathbb{V}(\alpha(\mathfrak{s}))$ is \mathfrak{J}_l , THEN

$$\begin{cases} \dot{x}(\alpha(\mathfrak{s})) &= \mathbf{A}_{\varphi_1}x(\alpha(\mathfrak{s})) + \mathbf{B}_{\varphi_1}u(\alpha(\mathfrak{s})) + \mathbf{C}_{\varphi_1}\mathbb{V}(\alpha(\mathfrak{s})), \\ y(\mathfrak{s}) &= \mathbf{E}_{\varphi_1}x(\alpha(\mathfrak{s})) + \mathbf{D}_{\varphi_1}u(\alpha(\mathfrak{s})), i, l = 1, 2 \end{cases} \quad (8)$$

where $\varphi_1 = 1, 2, \dots, m$, ($m = 4$) is the number of IF-THEN fuzzy rules. $u(\alpha(\mathfrak{s})) \in \mathbb{R}^n$ and $x(\alpha(\mathfrak{s})) \in \mathbb{R}^m$ represent the control information and the state vectors, while $y(\mathfrak{s})$ stands for the system output. And then, $\mathbb{V}(\alpha(\mathfrak{s}))$ and $\eta(\alpha(\mathfrak{s}))$

denote the premise variables and $\mathfrak{J}_l, \mathfrak{F}_i$ are the related fuzzy sets. This fuzzy system can be expressed using the fuzzy inference method as follows:

$$\begin{cases} \dot{x}(\alpha(\mathfrak{s})) &= \sum_{\varphi_1=1}^m \Delta_{\varphi_1}(\varsigma) [\mathbf{A}_{\varphi_1} x(\alpha(\mathfrak{s})) + \mathbf{B}_{\varphi_1} u(\alpha(\mathfrak{s})) + \mathbf{C}_{\varphi_1} \mathbb{V}(\alpha(\mathfrak{s}))], \\ y(\mathfrak{s}) &= \sum_{\varphi_1=1}^m \Delta_{\varphi_1}(\varsigma) [\mathbf{E}_{\varphi_1} x(\alpha(\mathfrak{s})) + \mathbf{D}_{\varphi_1} u(\alpha(\mathfrak{s}))], i, l = 1, 2 \end{cases} \quad (9)$$

where $\Delta_{\varphi_1}(\varsigma) \geq 0, \sum_{\varphi_1=1}^m \Delta_{\varphi_1}(\varsigma) = 1$.

Using the event-triggered mechanism described in [35], all the sampled data transmitted to the controller is time-stamped and only transmitted when the following condition is unsatisfied:

$$e^T(\alpha(\mathfrak{s})) \Gamma_\iota e(\alpha(\mathfrak{s})) < \sigma x^T(\alpha(\mathfrak{s}_k)) \Gamma_\iota x(\alpha(\mathfrak{s}_k)), \quad (10)$$

$x(\alpha(\mathfrak{s})) - x(\alpha(\mathfrak{s}_k))$ are the current sampling instant and latest transmitted sampling instant, respectively, whereas $e(\alpha(\mathfrak{s}))$ is the error between them. Assuming Γ_ι are symmetric positive matrices, σ are given positive scalars.

Remark 2.1. [43] From (10), it can be seen that $\mathfrak{s}_{k+1}h$ determines the next release time

$$\mathfrak{s}_{k+1}h = \mathfrak{s}_k h + \min_{p \geq 1} \{ph | e^T(\alpha(\mathfrak{s}_k + p)h) \Gamma_\iota e(\alpha(\mathfrak{s}_k + p)h) \geq \sigma x^T(\alpha(\mathfrak{s}_{k+p})) \Gamma_\iota x(\alpha(\mathfrak{s}_{k+p}))\}, \quad (11)$$

where $e(\alpha(\mathfrak{s}_k + p)h) = x(\alpha(\mathfrak{s}_k + p)h) - x(\alpha(\mathfrak{s}_k)h)$. As a result, $\mathfrak{s}_{k+1}h - \mathfrak{s}_k h$ represents the transmission interval, and the sampled-data obtained by sensors during $[\mathfrak{s}_k h, \mathfrak{s}_{k+1}h]$ isn't transmitted to the controller fully, resulting in reduced bandwidth consumption with an event-triggered control scheme. $\sigma > 0$ is the coefficient of the threshold, $\{\alpha(\mathfrak{s}_k + p)h\}$ is the set of sampling instants during $[\mathfrak{s}_k h, \mathfrak{s}_{k+1}h]$, $p \in \mathbb{N}$, and $\Gamma_\iota > 0$ is a weighting matrix.

Remark 2.2. [25] The condition (10), when set to zero, will not always be satisfied if $\sigma = 0$. Event-triggered control schemes degenerate into time-triggered schemes in this case. As a reminder, the following assumptions will be used next time.

Assumption 2.1:[5] Time-triggered sensors are assumed in the communication network with a trigger period h . Furthermore, controllers and actuators triggered by events are taken into consideration.

Assumption 2.2:[5] We consider the total network-induced delay to be $\tau_{\mathfrak{s}_k}$, which is bounded and satisfies $0 < \tau_{\mathfrak{s}_k} \leq \tau_M$, where τ_M is a known constant. At the actuator, a logic zero order holder (ZOH)'s holding time is $t \in \Gamma_k = [\mathfrak{s}_k h + \tau_{\mathfrak{s}_k}, \mathfrak{s}_{k+1} h + \tau_{\mathfrak{s}_{k+1}}]$, where $\mathfrak{s}_k h + \tau_{\mathfrak{s}_k}$ is the instant when the control data packet reaches the ZOH.

Under the above assumptions, when $t \in \tilde{\Gamma}_k = [\mathfrak{s}_k^n h + \tau_{\mathfrak{s}_{k+n}}, \mathfrak{s}_{k+1}^n h + \tau_{\mathfrak{s}_{k+n+1}}]$ the error between the future transmitted sampling instant $\mathfrak{s}_{k+1}h$ and the current transmitted sampling instant $\mathfrak{s}_k h$ can be deduced as

$$e(\alpha(\mathfrak{s}_k^n h)) = x(\alpha(\mathfrak{s}_k^n h)) - x(\alpha(\mathfrak{s}_k h)), \quad (12)$$

where $\alpha(\mathfrak{s}_k^n h) = \alpha(\mathfrak{s}_k h + nh)$ is the sampling instant between the above two states.

Define $\tau(\alpha(\mathfrak{s})) = \alpha(\mathfrak{s}) - \alpha(\mathfrak{s})_k^n h$, then the expression of the transmitted state $x(\alpha(\mathfrak{s})_k h)$ can be described as

$$x(\alpha(\mathfrak{s})_k h) = x(\alpha(\mathfrak{s}) - \tau(\alpha(\mathfrak{s}))) - e(\alpha(\mathfrak{s}_k^n h)). \quad (13)$$

In light of the above definition about $\tau(\alpha(\mathfrak{s}))$, it yields that $\dot{\tau}(\alpha(\mathfrak{s})) = 1$ for $t \in \Gamma_\iota$ and

$$0 < \tau_{\mathfrak{s}_k} \leq \tau_{\alpha(\mathfrak{s})} \leq h + \max \tau_{\mathfrak{s}_k}, \tau_{\mathfrak{s}_{k+1}} = h = \tau_M. \quad (14)$$

We are designing fuzzy-model based state feedback controllers as follows:

Control Rule φ_2 : IF $\eta(\alpha(\mathfrak{s}))$ is \mathfrak{F}_i , and $\mathbb{V}(\alpha(\mathfrak{s}))$ is \mathfrak{J}_l , THEN

$$u(\alpha(\mathfrak{s})) = K_{\varphi_2} x(\alpha(\mathfrak{s}_k h)), t \in [\mathfrak{s}_k h + \tau_{\mathfrak{s}_k}, \mathfrak{s}_{k+1} h + \tau_{\mathfrak{s}_{k+1}}], \quad (15)$$

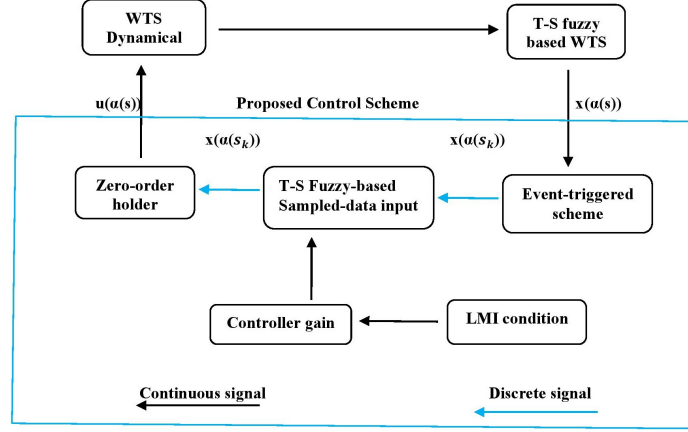


Figure 2: Proposed control scheme for T-S fuzzy wind turbine system

where K_{φ_2} are the desired controller gains to be determined for each $\varphi_2 = 1, 2, \dots, q$. The schematic diagram of event-triggered control framework is depicted in Figure 2. Then, the overall fuzzy controller could be rescheduled by

$$u(\alpha(\mathfrak{s})) = \sum_{\varphi_2=1}^m \Delta_{\varphi_2}(\varsigma) K_{\varphi_2} x(\alpha(\mathfrak{s}_k h)), t \in [\mathfrak{s}_k h + \tau_{\mathfrak{s}_k}, \mathfrak{s}_{k+1} h + \tau_{\mathfrak{s}_{k+1}}). \quad (16)$$

Substituting (13) into (16), we can obtain

$$u(\alpha(\mathfrak{s})) = \sum_{\varphi_2=1}^m \Delta_{\varphi_2}(\varsigma) K_{\varphi_2} [x(\alpha(\mathfrak{s})) - \tau(\alpha(\mathfrak{s})) - e(\alpha(\mathfrak{s}_k^n h))]. \quad (17)$$

Remark 2.3. [39] *There is an implicit assumption in most existing work concerning T-S fuzzy systems for wind turbines that premise variables should be consistent with fuzzy models. Then the fuzzy controller is chosen as $u(\alpha(\mathfrak{s})) = \sum_{\varphi_2=1}^m \Delta_{\varphi_2}(\varsigma) K_{\varphi_2} x(\alpha(\mathfrak{s}_k h))$. Despite this, the controller and plant membership functions in wind turbine T-S fuzzy systems are no longer equivalent due to sampling behaviors and network environment influences. This work chooses the designed controller as the representation of (17), rather than $u(\alpha(\mathfrak{s})) = \sum_{\varphi_2=1}^m \Delta_{\varphi_2}(\varsigma) K_{\varphi_2} x(\alpha(\mathfrak{s}_k h))$.*

Combining (10)-(16) and substituting (17) into (9), the closed-loop fuzzy system (CLFS) (Σ) could be rearranged as

$$\begin{cases} \dot{x}(\alpha(\mathfrak{s})) &= \Upsilon_{\varphi_1} \Upsilon_{\varphi_2} [\mathbf{A}_{\varphi_1} x(\mathfrak{s}) + \mathbf{B}_{\varphi_1} K_{\varphi_2} x(\mathfrak{s} - \tau(\mathfrak{s})) - \mathbf{B}_{\varphi_1} K_{\varphi_2} e(\mathfrak{s}_k^n h) + \mathbf{C}_{\varphi_1} \mathbb{V}(\mathfrak{s})], \\ y(\mathfrak{s}) &= \Upsilon_{\varphi_1} \Upsilon_{\varphi_2} [\mathbf{E}_{\varphi_1} x(\mathfrak{s}) + \mathbf{D}_{\varphi_1} K_{\varphi_2} x(\mathfrak{s} - \tau(\mathfrak{s})) - \mathbf{D}_{\varphi_1} K_{\varphi_2} e(\mathfrak{s}_k^n h)], \end{cases} \quad (18)$$

where $\Upsilon_{\varphi_1} = \sum_{\varphi_1=1}^m \Delta_{\varphi_1}(\varsigma)$, $\Upsilon_{\varphi_2} = \sum_{\varphi_2=1}^m \Delta_{\varphi_2}(\varsigma)$.

3 Definition and lemmas

Definition 3.1. [8] *Given a scalar $\gamma > 0$, then the closed loop system (18) is asymptotically stable and satisfies the given H_∞ performance index, if the following condition under zero initial conditions holds for all non-zero $\mathbb{V}(\mathfrak{s}) \in L_2[0, \infty)$,*

$$\sum_{t=0}^{\infty} y^s(\mathfrak{s}) y(\mathfrak{s}) < \gamma^2 \sum_{t=0}^{\infty} \mathbb{V}(\mathfrak{s})^T \mathbb{V}(\mathfrak{s}). \quad (19)$$

Lemma 3.2. (Schur Complement)[20] *Given constant matrices \mathcal{Y}_1 , \mathcal{Y}_2 and \mathcal{Y}_3 with appropriate dimensions, where $\mathcal{Y}_1^T = \mathcal{Y}_1$ and $\mathcal{Y}_2^T = \mathcal{Y}_2 > 0$, then $\mathcal{Y}_1 - \mathcal{Y}_3^T \mathcal{Y}_2^{-1} \mathcal{Y}_3 > 0$ if and only if*

$$\begin{bmatrix} \mathcal{Y}_1 & \mathcal{Y}_3 \\ \mathcal{Y}_3^T & \mathcal{Y}_2 \end{bmatrix} > 0. \quad (20)$$

Lemma 3.3. [45] *For any constant matrix $\mathfrak{U} > 0$, the following inequality holds for all continuously differentiable function $\rho(\cdot)$ in $[a, b] \rightarrow \mathbb{R}^n$*

$$-(q-p) \int_p^q \dot{\rho}(s) \mathbb{H} \dot{\rho}(s) ds \leq -(\rho(q) - \rho(p))^T \mathbb{H} (\rho(q) - \rho(p)) - 3\xi^T \mathbb{H} \xi,$$

where $\xi = (\rho(q) + \rho(p)) - [\frac{2}{(q-p)}] \int_p^q \rho(s) ds$.

Lemma 3.4. [46] *Let \mathcal{G} and \mathcal{H} be real matrices of appropriate dimensions. For a given scalar $\mu > 0$, and vectors $x, y \in \mathbb{R}^n$, we have:*

$$2x^T \mathcal{G}^T \mathcal{H} y \leq \mu^{-1} x^T \mathcal{G}^T \mathcal{G} x + \mu y^T \mathcal{H}^T \mathcal{H} y. \quad (21)$$

4 Main result

Developing a controller design method will be the focus of this section. The event-based asynchronous control loop systems (18) will be discussed.

Theorem 4.1. *Given positive constants $\epsilon_1, \epsilon_2, \epsilon_3$ and $0 < \tau_{s_k} \leq \tau_M$, and event-triggered state-feedback controller gain matrices K_{φ_2} , the closed loop T-S fuzzy system (18) is said to be asymptotically stable and satisfies the given H_∞ performance index, if there exist matrices $\mathbb{P} > 0$, $\mathbb{Q}_i > 0$ and $\mathbb{S}_i > 0$ for all $i \in \{1, 2\}$ such that the following LMIs are holds:*

$$\hat{\Xi} = \begin{bmatrix} \hat{\Xi}_{aa} & \hat{\Xi}_{ab} \\ * & \hat{\Xi}_{bb} \end{bmatrix} < 0, \quad (22)$$

where

$$\hat{\Xi}_{aa} = \begin{bmatrix} \hat{\Xi}_{11} & \hat{\Xi}_{12} & 0 & \mathbf{C}_{\varphi_1} \mathbb{P} & \hat{\Xi}_{15} & 6\mathbb{S}_1 & 0 & \mathbf{A}_{\varphi_1} \\ * & \hat{\Xi}_{22} & -4\mathbb{S}_2 & 0 & 0 & 6\mathbb{S}_1 & 6\mathbb{S}_2 & \mathbf{B}_{\varphi_1} K_{\varphi_2} \\ * & * & \hat{\Xi}_{33} & 0 & 0 & 0 & 6\mathbb{S}_2 & 0 \\ * & * & * & -\Gamma_\iota & 0 & 0 & 0 & \mathbf{C}_{\varphi_1} \\ * & * & * & * & -\gamma^2 I & 0 & 0 & -\mathbf{B}_{\varphi_1} K_{\varphi_2} \\ * & * & * & * & * & -12\mathbb{S}_1 & 0 & 0 \\ * & * & * & * & * & * & -12\mathbb{S}_2 & 0 \\ * & * & * & * & * & * & * & -\frac{1}{\tau(\mathfrak{s})} \mathbb{S}_1^{-1} \end{bmatrix},$$

$$\hat{\Xi}_{ab} = \begin{bmatrix} \mathbf{A}_{\varphi_1} & \mathbf{E}_{\varphi_1}^T \\ \mathbf{B}_{\varphi_1} K_{\varphi_2} & \mathbf{D}_{\varphi_1}^T K_{\varphi_2}^T \\ 0 & 0 \\ \mathbf{C}_{\varphi_1} & 0 \\ -\mathbf{B}_{\varphi_1} K_{\varphi_2} & -\mathbf{D}_{\varphi_1}^T K_{\varphi_2}^T \end{bmatrix}, \hat{\Xi}_{bb} = \begin{bmatrix} \hat{\Xi}_{99} & 0 \\ * & -I \end{bmatrix},$$

$$\hat{\Xi}_{11} = 2\mathbf{A}_{\varphi_1} \mathbb{P} + \mathbb{Q}_1 + 4\mathbb{S}_1,$$

$$\hat{\Xi}_{12} = \mathbf{B}_{\varphi_1} K_{\varphi_2} \mathbb{P} + 4\mathbb{S}_1,$$

$$\hat{\Xi}_{15} = -\mathbf{B}_{\varphi_1} K_{\varphi_2} \mathbb{P}$$

$$\hat{\Xi}_{22} = -\mathbb{Q}_1 + \mathbb{Q}_2 - 4\mathbb{S}_1 - 4\mathbb{S}_2,$$

$$\hat{\Xi}_{33} = -\mathbb{Q}_2 - 4\mathbb{S}_2 + \sigma \Gamma_\iota,$$

$$\hat{\Xi}_{99} = -\frac{1}{\tau_M - \tau(\mathfrak{s})} \mathbb{S}_2^{-1}.$$

Proof. Construct a Lyapunov-Krasovskii functional as follows:

$$\mathcal{V}(\mathfrak{s}) = \sum_{\kappa=1}^4 \mathcal{V}_\kappa(\mathfrak{s}), \quad (23)$$

$$\begin{aligned}
\mathcal{V}_a(\mathfrak{s}) &= x^T(\mathfrak{s})\mathbb{P}x(\mathfrak{s}), \\
\mathcal{V}_b(\mathfrak{s}) &= \int_{\mathfrak{s}-\tau(\mathfrak{s})}^{\mathfrak{s}} x^T(\mu)\mathbb{Q}_1x(\mu)d\mu + \int_{\mathfrak{s}-\tau_M}^{\mathfrak{s}-\tau(\mathfrak{s})} x^T(\mu)\mathbb{Q}_2x(\mu)d\mu, \\
\mathcal{V}_c(\mathfrak{s}) &= \int_{\mathfrak{s}-\tau(\mathfrak{s})}^{\mathfrak{s}} \int_{\theta}^{\mathfrak{s}} \dot{x}^T(\mu)\mathbb{S}_1\dot{x}(\mu)d\mu d\theta, \\
\mathcal{V}_d(\mathfrak{s}) &= (\tau_M - \tau(\mathfrak{s})) \int_{\mathfrak{s}-\tau_M}^{\mathfrak{s}-\tau(\mathfrak{s})} \int_{\theta}^{\mathfrak{s}} \dot{x}^T(\mu)\mathbb{S}_2\dot{x}(\mu)d\mu d\theta,
\end{aligned}$$

We define \mathcal{LV} as the weak infinitesimal generator, the time derivative of $V(\mathfrak{s})$ along the trajectory of (18) is given by

$$\begin{aligned}
\mathcal{LV}_a(\mathfrak{s}) &= 2\dot{x}^T(\mathfrak{s})\mathbb{P}x(\mathfrak{s}), \\
&= 2[\mathbf{A}_{\varphi_1}x(\mathfrak{s}) + \mathbf{B}_{\varphi_1}K_{\varphi_2}x(\mathfrak{s} - \tau(\mathfrak{s})) - \mathbf{B}_{\varphi_1}K_{\varphi_2}e(\mathfrak{s}_k^nh) + \mathbf{C}_{\varphi_1}\mathbb{V}(\mathfrak{s})]^T\mathbb{P}x(\mathfrak{s}), \\
\mathcal{LV}_b(\mathfrak{s}) &= x^T(\mathfrak{s})\mathbb{Q}_1x(\mathfrak{s}) - x^T(\mathfrak{s} - \tau(\mathfrak{s}))\mathbb{Q}_1x(\mathfrak{s} - \tau(\mathfrak{s})) + x^T(\mathfrak{s} - \tau(\mathfrak{s}))\mathbb{Q}_2x(\mathfrak{s} - \tau(\mathfrak{s})) \\
&\quad - x^T(\mathfrak{s} - \tau_M)\mathbb{Q}_2x(\mathfrak{s} - \tau_M), \\
\mathcal{LV}_c(\mathfrak{s}) &= \tau^2(\mathfrak{s})\dot{x}^T(\mathfrak{s})\mathbb{S}_1\dot{x}(\mathfrak{s}) - \tau(\mathfrak{s}) \int_{\mathfrak{s}-\tau(\mathfrak{s})}^{\mathfrak{s}} \dot{x}^T(\mu)\mathbb{S}_1\dot{x}(\mu)d\mu, \\
\mathcal{LV}_d(\mathfrak{s}) &= (\tau_M - \tau(\mathfrak{s}))^2\dot{x}^T(\mathfrak{s})\mathbb{S}_2\dot{x}(\mathfrak{s}) - (\tau_M - \tau(\mathfrak{s})) \int_{\mathfrak{s}-\tau_M}^{\mathfrak{s}-\tau(\mathfrak{s})} \dot{x}^T(\mu)\mathbb{S}_2\dot{x}(\mu)d\mu,
\end{aligned}$$

From Lemma 3.2,

$$\begin{aligned}
-\tau(\mathfrak{s}) \int_{\mathfrak{s}-\tau(\mathfrak{s})}^{\mathfrak{s}} \dot{x}^T(\mu)\mathbb{S}_1\dot{x}(\mu)d\mu &\leq - \left[\begin{array}{c} x(\mathfrak{s}) - x(\mathfrak{s} - \tau(\mathfrak{s})) \\ x(\mathfrak{s}) + x(\mathfrak{s} - \tau(\mathfrak{s})) - \frac{2}{\tau(\mathfrak{s})} \int_{\mathfrak{s}-\tau(\mathfrak{s})}^{\mathfrak{s}} x^T(\mu)d\mu \end{array} \right]^T \left[\begin{array}{cc} \mathbb{S}_1 & 0 \\ 0 & 3\mathbb{S}_1 \end{array} \right] \\
&\quad \left[\begin{array}{c} x(\mathfrak{s}) - x(\mathfrak{s} - \tau(\mathfrak{s})) \\ x(\mathfrak{s}) + x(\mathfrak{s} - \tau(\mathfrak{s})) - \frac{2}{\tau(\mathfrak{s})} \int_{\mathfrak{s}-\tau(\mathfrak{s})}^{\mathfrak{s}} x(\mu)d\mu \end{array} \right], \tag{24}
\end{aligned}$$

$$\begin{aligned}
-(\tau_M - \tau(\mathfrak{s})) \int_{\mathfrak{s}-\tau_M}^{\mathfrak{s}-\tau(\mathfrak{s})} \dot{x}^T(\mu)\mathbb{S}_2\dot{x}(\mu)d\mu &\leq - \left[\begin{array}{c} x(\mathfrak{s} - \tau(\mathfrak{s})) - x(\mathfrak{s} - \tau_M) \\ x(\mathfrak{s} - \tau(\mathfrak{s})) - x(\mathfrak{s} - \tau_M) - \frac{2}{\tau_M - \tau(\mathfrak{s})} \int_{\mathfrak{s}-\tau(\mathfrak{s})}^{\mathfrak{s}-\tau_M} x(\mu)d\mu \end{array} \right]^T \\
&\quad \left[\begin{array}{cc} \mathbb{S}_2 & 0 \\ 0 & 3\mathbb{S}_2 \end{array} \right] \left[\begin{array}{c} x(\mathfrak{s} - \tau(\mathfrak{s})) - x(\mathfrak{s} - \tau_M) \\ x(\mathfrak{s} - \tau(\mathfrak{s})) - x(\mathfrak{s} - \tau_M) - \frac{2}{\tau_M - \tau(\mathfrak{s})} \int_{\mathfrak{s}-\tau(\mathfrak{s})}^{\mathfrak{s}-\tau_M} x(\mu)d\mu \end{array} \right], \tag{25}
\end{aligned}$$

From (23)-(25), we get

$$\mathcal{LV}(\mathfrak{s}) = \zeta^T(\mathfrak{s})\Xi_{7 \times 7}\zeta(\mathfrak{s}) + \dot{x}^T(\mathfrak{s})[\tau(\mathfrak{s})^2\mathbb{S}_1 + (\tau_M - \tau(\mathfrak{s}))^2\mathbb{S}_2]\dot{x}(\mathfrak{s}), \tag{26}$$

where

$$\zeta(\mathfrak{s}) = \left[\begin{array}{cccccc} x(\mathfrak{s}) & x(\mathfrak{s} - \tau(\mathfrak{s})) & x(\mathfrak{s} - \tau_M) & e(t_k^nh) & \mathbb{V}(\mathfrak{s}) & \frac{1}{\tau_M - \tau(\mathfrak{s})} \int_{\mathfrak{s}-\tau_M}^{\mathfrak{s}-\tau(\mathfrak{s})} x(\mu)d\mu & \frac{1}{\tau_M} \int_{\mathfrak{s}-\tau_M}^{\mathfrak{s}} x(\mu)d\mu \end{array} \right]^T$$

$$\Xi_{16} = 6\mathbb{S}_1, \quad \Xi_{26} = 6\mathbb{S}_1, \quad \Xi_{27} = 6\mathbb{S}_2, \quad \Xi_{37} = 6\mathbb{S}_2, \quad \Xi_{66} = -12\mathbb{S}_1, \quad \Xi_{77} = -12\mathbb{S}_2, \quad \Xi_{23} = 2\mathbb{S}_2,$$

$$\Xi_{11} = 2\mathbf{A}_{\varphi_1}\mathbb{P} + \mathbb{Q}_1 + 4\mathbb{S}_1,$$

$$\Xi_{12} = \mathbf{B}_{\varphi_1}K_{\varphi_2}\mathbb{P} + 2\mathbb{S}_1,$$

$$\Xi_{14} = \mathbf{C}_{\varphi_1}\mathbb{P},$$

$$\Xi_{15} = -\mathbf{B}_{\varphi_1}K_{\varphi_2}\mathbb{P},$$

$$\Xi_{22} = -\mathbb{Q}_1 + \mathbb{Q}_2 - 4\mathbb{S}_1 - 4\mathbb{S}_2,$$

$$\Xi_{33} = -\mathbb{Q}_2 - 4\mathbb{S}_2.$$

other Ξ_{ij} terms are zero. To show the closed-loop system (18) has H_∞ performance γ , we introduce the following index

$$\mathcal{J}(\mathfrak{s}) = \int_0^\infty [W(y^T(\mathfrak{s}), \mathbb{V}(\mathfrak{s})) - \gamma^2\mathbb{V}^T(\mathfrak{s})\mathbb{V}(\mathfrak{s})]dt. \tag{27}$$

Under the zero initial condition, we can obtain

$$\begin{aligned}\mathcal{J}(\mathfrak{s}) &= \int_0^\infty [y^T(\mathfrak{s})y(\mathfrak{s}) - \gamma^2 \mathbb{V}^T(\mathfrak{s})\mathbb{V}(\mathfrak{s}) + \mathcal{L}\mathcal{V}(\mathfrak{s})]dt - V(\infty) \\ &= \zeta^T(\mathfrak{s})\Xi_{7 \times 7}\zeta(\mathfrak{s}) + (\mathbf{E}_{\varphi_1}x(\mathfrak{s}) + \mathbf{D}_{\varphi_1}K_{\varphi_2}x(\mathfrak{s} - \tau(\mathfrak{s})) - \mathbf{D}_{\varphi_1}K_{\varphi_2}e(\mathfrak{s}_k^n h))^T \\ &\quad (\mathbf{E}_{\varphi_1}x(\mathfrak{s}) + \mathbf{D}_{\varphi_1}K_{\varphi_2}x(\mathfrak{s} - \tau(\mathfrak{s})) - \mathbf{D}_{\varphi_1}K_{\varphi_2}e(\mathfrak{s}_k^n h)) - \gamma^2 \mathbb{V}^T(\mathfrak{s})\mathbb{V}(\mathfrak{s}) \\ &\quad + \dot{x}^T(\mathfrak{s})[\tau(\mathfrak{s})^2 \mathbb{S}_1 + (\tau_M - \tau(\mathfrak{s}))^2 \mathbb{S}_2]\dot{x}(\mathfrak{s}).\end{aligned}$$

Finally, by applying Schur's complement inequality applied in (27), we get $\hat{\Xi} < 0$. This completes the proof. \square

Theorem 4.2. *Given positive constants $\epsilon_1, \epsilon_2, \epsilon_3$ and $0 < \tau_{s_k} \leq \tau_M$, the closed loop T-S fuzzy system (18) is said to be asymptotically stable and satisfies the given H_∞ performance, under the event-trigger scheme (10), if there exist matrices $\mathbb{X} > 0, \mathbb{Q}_i > 0, \mathbb{S}_i > 0$ and $\gamma > 0$ for all $i \in \{1, 2\}$ such that the following LMIs are holds:*

$$\hat{\Xi} = \begin{bmatrix} \hat{\Xi}_{aa} & \hat{\Xi}_{ab} \\ * & \hat{\Xi}_{bb} \end{bmatrix} < 0, \quad (28)$$

where

$$\hat{\Xi}_{aa} = \begin{bmatrix} \hat{\Xi}_{11} & \hat{\Xi}_{12} & \hat{\Xi}_{13} & \hat{\Xi}_{14} & 4\mathbb{S}_1 & 4\mathbb{S}_1 & 0 & 0 & 0 & 0 & 6\mathbb{S}_1 \\ * & \hat{\Xi}_{22} & \hat{\Xi}_{23} & \hat{\Xi}_{24} & 4\mathbb{S}_1 & 4\mathbb{S}_1 & \hat{\Xi}_{27} & 0 & 0 & 0 & 6\mathbb{S}_1 \\ * & * & \hat{\Xi}_{33} & \hat{\Xi}_{34} & 4\mathbb{S}_1 & \hat{\Xi}_{36} & 0 & 0 & 0 & \hat{\Xi}_{310} & 6\mathbb{S}_1 \\ * & * & * & \hat{\Xi}_{44} & \hat{\Xi}_{45} & 4\mathbb{S}_1 & 0 & 0 & \frac{1}{l}Y & 0 & 6\mathbb{S}_1 \\ * & * & * & * & \hat{\Xi}_{55} & \hat{\Xi}_{56} & -4\mathbb{S}_2 & 0 & 0 & 0 & 6\mathbb{S}_2 \\ * & * & * & * & * & \hat{\Xi}_{66} & -4\mathbb{S}_2 & 0 & 0 & 0 & 6\mathbb{S}_1 \\ * & * & * & * & * & * & \hat{\Xi}_{77} & 0 & 0 & 0 & 0 \\ * & * & * & * & * & * & * & -\Gamma_l & 0 & 0 & 0 \\ * & * & * & * & * & * & * & * & -\gamma^2 I & 0 & 0 \\ * & * & * & * & * & * & * & * & * & -\gamma^2 I & 0 \\ * & * & * & * & * & * & * & * & * & * & -12\mathbb{S}_1 \end{bmatrix},$$

$$\hat{\Xi}_{ab} = \begin{bmatrix} 0 & 0 & P & -P & 0 & 0 & P & -P & 0 & 0 & 0 \\ 0 & \hat{\Xi}_{213} & \hat{\Xi}_{214} & \hat{\Xi}_{215} & \hat{\Xi}_{216} & \hat{\Xi}_{217} & \hat{\Xi}_{218} & \hat{\Xi}_{219} & \hat{\Xi}_{220} & 0 & 0 \\ 0 & \hat{\Xi}_{313} & \hat{\Xi}_{314} & \hat{\Xi}_{315} & 0 & \hat{\Xi}_{317} & \hat{\Xi}_{318} & \hat{\Xi}_{319} & 0 & P & \hat{\Xi}_{322} \\ 0 & 0 & 0 & 0 & -\frac{1}{l}P & 0 & 0 & 0 & -\frac{1}{l}P & 0 & 0 \\ 6\mathbb{S}_2 & 0 & 0 & 0 & -\frac{1}{l}Y & 0 & 0 & 0 & -\frac{1}{l}Y & 0 & \hat{\Xi}_{522} \\ 6\mathbb{S}_2 & 0 & 0 & \hat{\Xi}_{615} & 0 & 0 & 0 & \hat{\Xi}_{619} & 0 & 0 & 0 \\ 6\mathbb{S}_2 & 0 & 0 & 0 & 0 & 0 & 0 & 0 & 0 & 0 & 0 \\ 0 & 0 & \hat{\Xi}_{814} & 0 & 0 & 0 & \hat{\Xi}_{818} & 0 & 0 & 0 & 0 \\ 0 & 0 & 0 & 0 & -\frac{1}{l}Y & 0 & 0 & 0 & -\frac{1}{l}Y & 0 & \hat{\Xi}_{922} \\ 0 & 0 & 0 & \hat{\Xi}_{1015} & 0 & 0 & 0 & \hat{\Xi}_{1019} & 0 & 0 & 0 \\ 0 & 0 & 0 & 0 & 0 & 0 & 0 & 0 & 0 & 0 & 0 \end{bmatrix},$$

$$\hat{\Xi}_{bb} = \text{diag}\{-12\mathbb{S}_2, \hat{\Xi}_{1313}, \hat{\Xi}_{1414}, \hat{\Xi}_{1515}, \hat{\Xi}_{1616}, \hat{\Xi}_{1717}, \hat{\Xi}_{1818}, \hat{\Xi}_{1919}, \hat{\Xi}_{2020}, -I, -I\}$$

$$\begin{aligned}\hat{\Xi}_{11} &= \hat{\Xi}_{14} = \mathbb{Q}_1 + 4\mathbb{S}_1, & \hat{\Xi}_{213} &= \hat{\Xi}_{217} = -\frac{\mathbf{N}_l}{\mathbf{G}_g}P, & \hat{\Xi}_{215} &= \hat{\Xi}_{219} = \frac{\mathbf{M}_g}{\mathbf{G}_r}P, \\ \hat{\Xi}_{216} &= \hat{\Xi}_{220} = \frac{\mathbb{J}_r \eta(\varsigma)}{\mathbf{G}_r}P, & \hat{\Xi}_{313} &= \hat{\Xi}_{317} = \frac{\mathbf{N}_l}{\mathbf{G}_g}P, & \hat{\Xi}_{314} &= \hat{\Xi}_{318} = \frac{\mathbf{M}_l}{\mathbf{G}_g}P, \\ \hat{\Xi}_{315} &= \hat{\Xi}_{319} = -\frac{(\mathbf{M}_l + \mathbf{M}_g)}{\mathbf{G}_g}P, & \hat{\Xi}_{1015} &= \hat{\Xi}_{1019} = -\frac{\mathbf{M}_g}{\mathbf{G}_g}Y, & \hat{\Xi}_{615} &= \hat{\Xi}_{619} = -\frac{\mathbf{M}_g}{\mathbf{G}_g}Y, \\ \hat{\Xi}_{814} &= \hat{\Xi}_{818} = \frac{\mathbb{J}_r \mathbb{V}(\varsigma)}{\mathbf{G}_g}P, & \hat{\Xi}_{214} &= \hat{\Xi}_{218} = -2\frac{\mathbb{J}_r \Psi_R(\varsigma) + \mathbf{M}_l}{\mathbf{G}_r}P, & \hat{\Xi}_{36} &= \frac{\mathbf{M}_g}{\mathbf{G}_g}Y + 4\mathbb{S}_1,\end{aligned}$$

$$\begin{aligned}
\tilde{\Xi}_{77} &= -4\mathbb{S}_1 - \mathbb{Q}_2 + \sigma\Gamma_\iota, & \tilde{\Xi}_{922} &= \mathbf{M}_\iota^T \mathbf{Y}^T, & \tilde{\Xi}_{44} &= -\frac{2}{\iota}\mathbb{P} + \mathbb{Q}_1 + 4\mathbb{S}_1, \\
\tilde{\Xi}_{45} &= \frac{1}{\iota}\mathbf{Y} + 4\mathbb{S}_1, & \tilde{\Xi}_{522} &= -\mathbf{M}_\iota^T \mathbf{Y}^T, & \tilde{\Xi}_{310} &= -\frac{\mathbf{M}_g}{\mathbf{G}_g} \mathbf{Y}, \\
\tilde{\Xi}_{34} &= \mathbb{Q}_1 + 4\mathbb{S}_1, & \tilde{\Xi}_{66} &= -\mathbb{Q}_1 - 4\mathbb{S}_1 + \mathbb{Q}_2 - 4\mathbb{S}_2, & \tilde{\Xi}_{12} &= \mathbb{P}^T - \frac{\mathbf{N}_\iota}{\mathbf{G}_r} \mathbb{P} + \mathbb{Q}_1 + 4\mathbb{S}_1, \\
\tilde{\Xi}_{33} &= -2\frac{(\mathbf{M}_\iota + \mathbf{M}_g)}{\mathbf{G}_g} \mathbb{P} + \mathbb{Q}_1 + 4\mathbb{S}_1, & \tilde{\Xi}_{55} &= \tilde{\Xi}_{56} = -\mathbb{Q}_1 - 4\mathbb{S}_1 + \mathbb{Q}_2 - 4\mathbb{S}_2, \\
\tilde{\Xi}_{22} &= -2\frac{\mathbb{J}_r \Psi_{\mathbf{R}}(\varsigma) + \mathbf{M}_\iota}{\mathbf{G}_r} \mathbb{P} + \mathbb{Q}_1 + 4\mathbb{S}_1, & \tilde{\Xi}_{13} &= -\mathbb{P}^T - \frac{\mathbf{N}_\iota}{\mathbf{G}_g} \mathbb{P} + \mathbb{Q}_1 + 4\mathbb{S}_1, \\
\tilde{\Xi}_{24} &= 2\frac{\mathbb{J}_r \eta(\varsigma)}{\mathbf{G}_r} \mathbb{P} + \mathbb{Q}_1 + 4\mathbb{S}_1, & \tilde{\Xi}_{23} &= \frac{\mathbf{M}_g}{\mathbf{G}_g} \mathbb{P} + \frac{\mathbf{M}_g^T}{\mathbf{G}_g^T} \mathbb{P}^T + \mathbb{Q}_1 + 4\mathbb{S}_1, \\
\tilde{\Xi}_{1313} &= \tilde{\Xi}_{1414} = \tilde{\Xi}_{1515} = \tilde{\Xi}_{1616} = -\frac{1}{\tau(\mathfrak{s})} (\mathbb{S}_1^{-1} - \mathbb{P} - \mathbb{P}^T), \\
\tilde{\Xi}_{1717} &= \tilde{\Xi}_{1818} = \tilde{\Xi}_{1919} = \tilde{\Xi}_{2020} = -\frac{1}{(\tau_M - \tau(\mathfrak{s}))} (\mathbb{S}_2^{-1} - \mathbb{P} - \mathbb{P}^T).
\end{aligned}$$

Proof. Now, we define

$$\mathbf{X} = \mathbb{P}, \quad \mathbf{Y} = \mathbf{K}\mathbb{P}^{-1}.$$

Pre and post multiplying by $\text{diag}\{I, I, I, I, X, I, X, X, X, X, I\}$ and its transpose, respectively. Then by using Schur's complement formula and the inequalities $-\mathbf{X}\mathbb{S}\mathbf{X} \leq \mathbb{S}^{-1} - 2\mathbf{X}$, one can see that the inequalities (20) gives (24).

Then, by substituting \mathbf{A}_{φ_1} , \mathbf{B}_{φ_1} , \mathbf{C}_{φ_1} , \mathbf{D}_{φ_1} , \mathbf{E}_{φ_1} in inequality (24), we get (30). Thus proof is completed. \square

Remark 4.3. [40] *It should be noted that the dissipative-based event-triggered control mechanism presented in this study is general and can be implemented in other practical systems, as well as active vehicle suspension systems [42], truck trailer models [11], multi-machine power systems [37], basic buck converters system [19] and so on. The variable speed Wind turbine systems under investigation is one possible practical system in engineering.*

5 Numerical example

In this section, we will implement the proposed control scheme into the variable-speed wind turbine system and chaotic Rossler's system to verify its effectiveness.

Example 5.1. *In order to illustrate the effectiveness of the proposed method, we consider the closed-loop fuzzy system (CLFS) (18) with the following data.*

$$\begin{cases} \dot{x}(\alpha(\mathfrak{s})) &= \Upsilon_{\varphi_1} \Upsilon_{\varphi_2} [\mathbf{A}_{\varphi_1} x(\mathfrak{s}) + \mathbf{B}_{\varphi_1} K_{\varphi_2} x(\mathfrak{s} - \tau(\mathfrak{s})) - \mathbf{B}_{\varphi_1} K_{\varphi_2} e(\mathfrak{s}_k^n \mathbf{h}) + \mathbf{C}_{\varphi_1} \mathbb{V}(\mathfrak{s})] \\ y(\mathfrak{s}) &= \Upsilon_{\varphi_1} \Upsilon_{\varphi_2} [\mathbf{E}_{\varphi_1} x(\mathfrak{s}) + \mathbf{D}_{\varphi_1} K_{\varphi_2} x(\mathfrak{s} - \tau(\mathfrak{s})) - \mathbf{D}_{\varphi_1} K_{\varphi_2} e(\mathfrak{s}_k^n \mathbf{h})]. \end{cases} \quad (29)$$

Then, the parameters and membership functions are described as follows: $h_1 = 0.3$, $h_2 = 0.5$, $h_3 = 5$, $f = 10$ and $\Upsilon_{\varphi_1}(x_1(\alpha(\mathfrak{s}))) = \frac{0.5}{f}(h_3 + f - x_1(\alpha(\mathfrak{s})))$ and $\Upsilon_{\varphi_2}(x_1(\alpha(\mathfrak{s}))) = 1 - \Upsilon_{\varphi_1}(x_1(\alpha(\mathfrak{s})))$.

The parameter matrices are given by $(\Sigma) = 2$:

$$\begin{aligned}
\mathbf{G}_{g_1} &= \begin{bmatrix} 0.41 & 0.2 \\ 0.3 & 0.51 \end{bmatrix}, \mathbf{G}_{g_2} = \begin{bmatrix} 0.41 & 0.5 \\ 0.9 & 0.51 \end{bmatrix}, \mathbf{G}_{r_1} = \begin{bmatrix} 3 & 1 \\ 0 & 1.8 \end{bmatrix}, \mathbf{G}_{r_2} = \begin{bmatrix} 3 & 1.2 \\ 0 & 2.3 \end{bmatrix}, \\
\mathbf{M}_{g_1} &= \begin{bmatrix} 2 & 0.5 \\ 0.1 & 3 \end{bmatrix}, \mathbf{M}_{g_2} = \begin{bmatrix} 2 & 0.6 \\ 0.4 & 3 \end{bmatrix}, \mathbf{M}_{s_1} = \begin{bmatrix} 0.03 & 1 \\ 3 & 4 \end{bmatrix}, \mathbf{M}_{s_2} = \begin{bmatrix} 2 & 1.6 \\ 4 & 2.6 \end{bmatrix}, \\
\mathbf{N}_{s_1} &= \begin{bmatrix} 2 & 1.5 \\ 3 & 0.1 \end{bmatrix}, \mathbf{N}_{s_2} = \begin{bmatrix} 2 & 2.5 \\ 3 & 0.3 \end{bmatrix}, \mathbb{V}_1 = \begin{bmatrix} 0.2 & 3 \\ 0.04 & 2 \end{bmatrix}, \mathbb{V}_2 = \begin{bmatrix} 0.7 & 3 \\ 0.4 & 2 \end{bmatrix}.
\end{aligned}$$

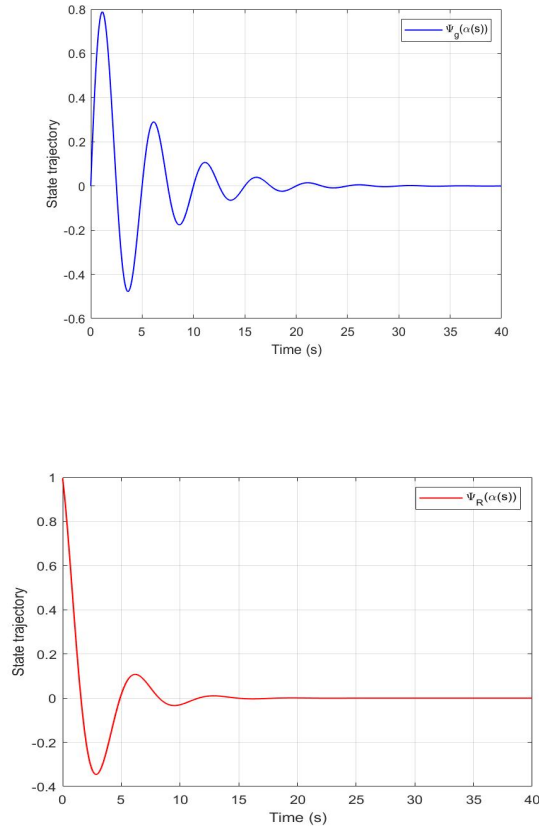
Let $\pi = 3.14$, $\rho = 1.225$, $r = 0.03$, $\iota = 0.05$, $\sigma = 0.01$, $\gamma = 0.06$, $\Lambda = 0.06$, $\tau_M = 0.03$ and $\tau(\mathfrak{s}) = 0.04$. By Theorem 4.2, the matrices of the controller are obtained as follows

$$\begin{aligned} \Gamma_1 &= \begin{bmatrix} 0.1208 & 0.0017 \\ 0.0017 & 0.1187 \end{bmatrix}, \Gamma_2 = \begin{bmatrix} 0.1185 & 0.0004 \\ 0.0004 & 0.1220 \end{bmatrix}, \mathbb{P}_1 = \begin{bmatrix} 0.0015 & 0.0007 \\ 0.0007 & 0.0018 \end{bmatrix}, \\ \mathbb{P}_2 &= \begin{bmatrix} 0.0009 & 0.0013 \\ 0.0013 & 0.0024 \end{bmatrix}, Q_{1_1} = \begin{bmatrix} -0.0217 & 0.0004 \\ 0.0004 & -0.0199 \end{bmatrix}, Q_{1_2} = \begin{bmatrix} -0.0214 & 0.0003 \\ 0.0003 & -0.0201 \end{bmatrix}, \\ Q_{2_1} &= \begin{bmatrix} -0.0159 & -0.0000 \\ -0.0000 & -0.0140 \end{bmatrix}, Q_{2_2} = \begin{bmatrix} -0.0158 & 0.0004 \\ 0.0004 & -0.0150 \end{bmatrix}, S_{1_1} = \begin{bmatrix} 0.0027 & 0.0000 \\ 0.0000 & 0.0026 \end{bmatrix}, \\ S_{1_2} &= \begin{bmatrix} 0.0026 & 0.0000 \\ 0.0000 & 0.0027 \end{bmatrix}, S_{2_1} = \begin{bmatrix} -0.0011 & 0.0000 \\ 0.0000 & -0.0011 \end{bmatrix}, S_{2_2} = \begin{bmatrix} -0.0011 & -0.0000 \\ -0.0000 & -0.0011 \end{bmatrix}, \\ Y_1 &= 1.0e - 03 * \begin{bmatrix} -0.1010 & 0.0440 \\ 0.0440 & -0.1184 \end{bmatrix}, Y_2 = 1.0e - 04 * \begin{bmatrix} -0.5166 & -0.2985 \\ -0.2985 & -0.0211 \end{bmatrix}. \end{aligned}$$

By solving the feasibility of the LMI-based conditions (28) and (29), we get the following control gain matrices.

$$K_1 = Y\mathbb{X}^{-1} = \begin{bmatrix} -0.0991 & 0.0665 \\ 0.0777 & -0.0998 \end{bmatrix}, K_2 = Y\mathbb{X}_2^{-1} = \begin{bmatrix} -0.1882 & 0.0900 \\ -0.1525 & 0.0822 \end{bmatrix}.$$

From Figure 4 it reveals that the proposed approaches maximal ranges of sampling period with the minimal number



of decision variables. By setting the initial values $\mathbb{V}(\mathfrak{s})$, the state response of system states and control responses of system (18) are presented in Figures 3 and 5 respectively. From Figure 5 we can observe that the system states tends to zero asymptotically. Under the consideration of gain matrices and initial values $\omega(\alpha(\mathfrak{s})) = [-0.1, 0.2, 0.3]^T$, the system states and control responses of the chaotic system [44] are depicted in Figure 3.

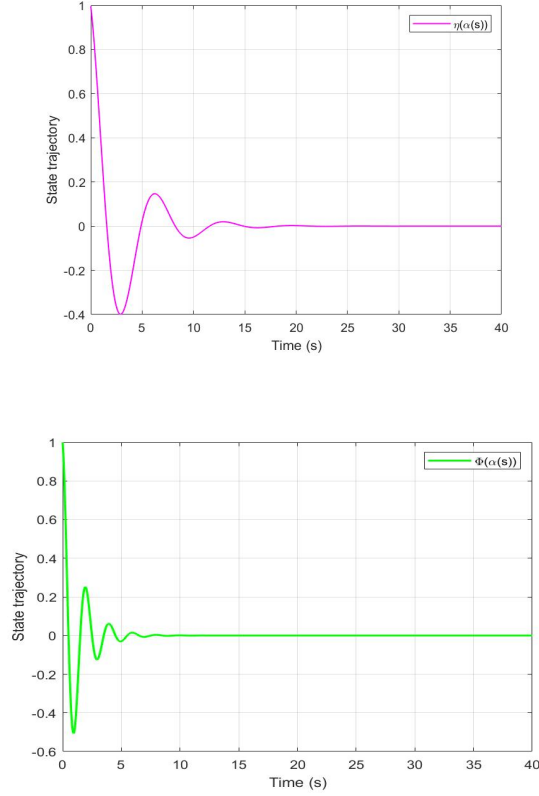


Figure 3: Time responses of system states $\Psi_R(\alpha(\mathfrak{s}))$, $\Psi_g(\alpha(\mathfrak{s}))$, $\Phi(\alpha(\mathfrak{s}))$ and $\eta(\alpha(\mathfrak{s}))$

Example 5.2. To demonstrate the superiority of the proposed control scheme with existing results, we will consider the well known chaotic system (Rossler system) (27) as follows:

$$\begin{cases} \dot{x}(\alpha(\mathfrak{s})) &= \Upsilon_{\varphi_1} \Upsilon_{\varphi_2} [\mathbf{A}_{\varphi_1} x(\mathfrak{s}) + \mathbf{B}_{\varphi_1} K_{\varphi_2} x(\mathfrak{s} - \tau(\mathfrak{s})) - \mathbf{B}_{\varphi_1} K_{\varphi_2} e(\mathfrak{s}_k^r \mathfrak{h}) + \mathbf{C}_{\varphi_1} \nabla(\mathfrak{s})] \\ y(\mathfrak{s}) &= \Upsilon_{\varphi_1} \Upsilon_{\varphi_2} [\mathbf{E}_{\varphi_1} x(\mathfrak{s}) + \mathbf{D}_{\varphi_1} K_{\varphi_2} x(\mathfrak{s} - \tau(\mathfrak{s})) - \mathbf{D}_{\varphi_1} K_{\varphi_2} e(\mathfrak{s}_k^r \mathfrak{h})]. \end{cases} \quad (30)$$

Then, the parameters and membership functions are described as follows: $h_1 = 0.4$, $h_2 = 0.5$, $h_3 = 5.5$, $f = 10$ and $\Upsilon_{\varphi_1}(x_1(\alpha(\mathfrak{s}))) = \frac{0.5}{f}(h_3 + f - x_1(\alpha(\mathfrak{s})))$ and $\Upsilon_{\varphi_2}(x_1(\alpha(\mathfrak{s}))) = 1 - \Upsilon_{\varphi_1}(x_1(\alpha(\mathfrak{s})))$.

The parameter matrices are given by (Σ):

$$\begin{aligned} \mathbf{G}_{\mathbf{g}_1} &= \begin{bmatrix} 0 & 4 & 1 \\ 0.5 & 0 & 9 \\ 1 & 5 & 2 \end{bmatrix}, \mathbf{G}_{\mathbf{g}_2} = \begin{bmatrix} 0 & 4 & 1.7 \\ 0.5 & 0 & 8 \\ 1 & 5 & 3 \end{bmatrix}, \mathbf{G}_{r_1} = \begin{bmatrix} 3 & 1 & 2 \\ 0 & 4 & 1 \\ 1.6 & 2 & 0.3 \end{bmatrix}, \\ \mathbf{G}_{r_2} &= \begin{bmatrix} 3.2 & 1 & 2.6 \\ 0 & 4 & 1 \\ 1.8 & 2 & 0.7 \end{bmatrix}, \mathbf{M}_{\mathbf{g}_1} = \begin{bmatrix} 2 & 0 & 6 \\ 0 & 4 & 3 \\ 5 & 1.6 & 0 \end{bmatrix}, \mathbf{M}_{\mathbf{g}_2} = \begin{bmatrix} 3 & 1 & 7 \\ 0 & 5 & 4 \\ 6 & 1.6 & 0 \end{bmatrix}, \\ \mathbf{M}_{s_1} &= \begin{bmatrix} 3 & 0 & 1.4 \\ 3 & 4 & 2 \\ 0 & 2 & 0 \end{bmatrix}, \mathbf{M}_{s_2} = \begin{bmatrix} 3.2 & 0 & 1.4 \\ 3 & 4.7 & 2 \\ 0 & 2 & 1 \end{bmatrix}, \mathbf{N}_{s_1} = \begin{bmatrix} 3 & 0 & 2.5 \\ 1 & 2 & 0.3 \\ 0 & 4 & 1.7 \end{bmatrix}, \\ \mathbf{N}_{s_2} &= \begin{bmatrix} 3 & 0.5 & 2 \\ 1 & 2.3 & 0.7 \\ 0 & 4 & 2 \end{bmatrix}, \mathbf{V}_1 = \begin{bmatrix} 0 & 7 & 3 \\ 1.2 & 4 & 2 \\ 1 & 0.2 & 6 \end{bmatrix}, \mathbf{V}_2 = \begin{bmatrix} 0 & 7.2 & 3 \\ 1.2 & 4.3 & 2 \\ 1 & 0.6 & 5 \end{bmatrix}. \end{aligned}$$

Let $\pi = 3.14$, $\rho = 1.226$, $r = 0.04$, $\iota = 0.06$, $\sigma = 0.02$, $\gamma = 0.1$, $\Lambda = 0.2$, $\tau_M = 0.05$ and $\tau(\mathfrak{s}) = 0.08$. By Theorem 4.2, the matrices of the controller are obtained as follows

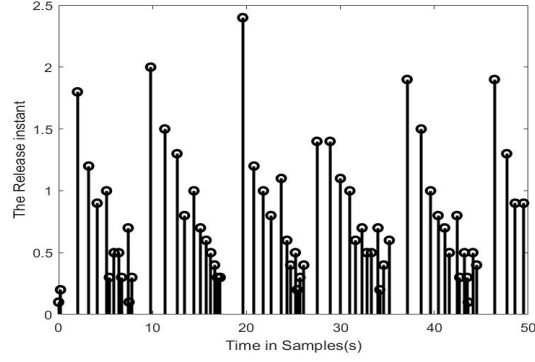


Figure 4: Fuzzy control with event-triggered strategy

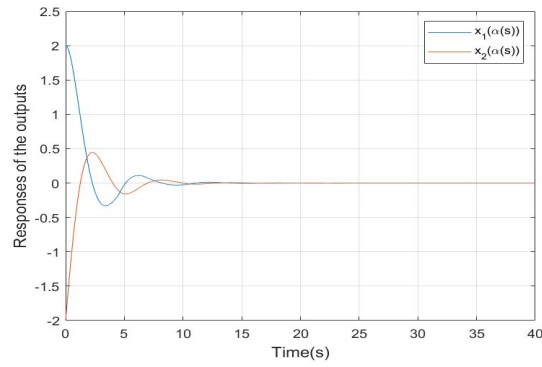
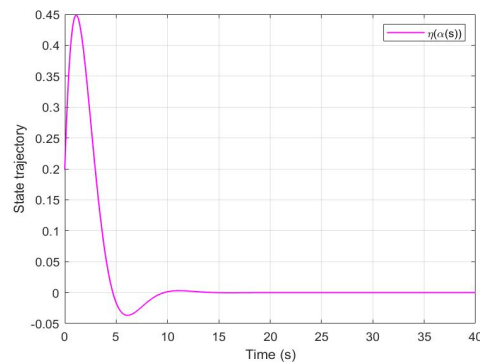
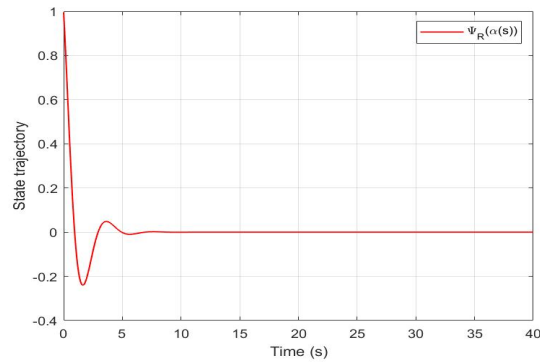
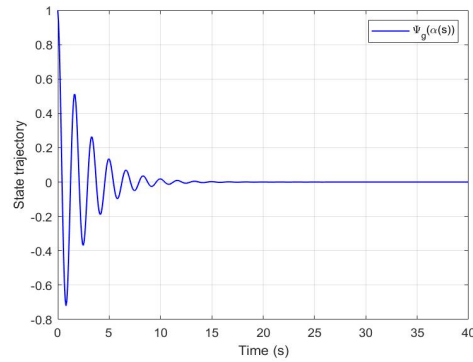


Figure 5: State trajectory of systems (29) is asymptotically stable

$$\begin{aligned}
 \mathbb{P}_1 &= \begin{bmatrix} 0.0011 & 0.0002 & 0.0010 \\ 0.0002 & 0.0031 & 0.0007 \\ 0.0010 & 0.0007 & 0.0029 \end{bmatrix}, \mathbb{P}_2 = \begin{bmatrix} 0.0010 & 0.0003 & 0.0010 \\ 0.0003 & 0.0029 & 0.0008 \\ 0.0010 & 0.0008 & 0.0026 \end{bmatrix}, \\
 Q_{11} &= \begin{bmatrix} -0.0232 & -0.0003 & 0.0010 \\ -0.0003 & -0.0227 & 0.0000 \\ 0.0010 & 0.0000 & -0.0222 \end{bmatrix}, Q_{12} = \begin{bmatrix} -0.0229 & -0.0001 & 0.0009 \\ -0.0001 & -0.0228 & 0.0002 \\ 0.0009 & 0.0002 & -0.0225 \end{bmatrix}, \\
 Q_{21} &= \begin{bmatrix} -0.0181 & -0.0001 & 0.0006 \\ -0.0001 & -0.0179 & 0.0000 \\ 0.0006 & 0.0000 & -0.0176 \end{bmatrix}, Q_{22} = \begin{bmatrix} -0.0180 & -0.0000 & 0.0005 \\ -0.0000 & -0.0179 & 0.0001 \\ 0.0005 & 0.0001 & -0.0177 \end{bmatrix}, \\
 S_{12} &= \begin{bmatrix} 0.0026 & 0.0000 & 0.0001 \\ 0.0000 & 0.0027 & 0.0001 \\ 0.0001 & 0.0001 & 0.0028 \end{bmatrix}, S_{11} = \begin{bmatrix} 0.0026 & -0.0000 & 0.0001 \\ -0.0000 & 0.0027 & 0.0000 \\ 0.0001 & 0.0000 & 0.0028 \end{bmatrix}, \\
 S_{21} &= \begin{bmatrix} -0.0011 & 0.0000 & -0.0000 \\ 0.0000 & -0.0011 & -0.0000 \\ -0.0000 & -0.0000 & -0.0011 \end{bmatrix}, S_{22} = \begin{bmatrix} -0.0011 & -0.0000 & -0.0000 \\ -0.0000 & -0.0011 & -0.0000 \\ -0.0000 & -0.0000 & -0.0011 \end{bmatrix}, \\
 Y_1 &= 1.0e-04 * \begin{bmatrix} -0.2322 & -0.1147 & 0.3265 \\ -0.1147 & -0.1410 & 0.1411 \\ 0.3265 & 0.1411 & -0.5957 \end{bmatrix}, \Gamma_1 = \begin{bmatrix} 0.2434 & -0.0003 & 0.0013 \\ -0.0003 & 0.2443 & 0.0001 \\ 0.0013 & 0.0001 & 0.2448 \end{bmatrix}, \\
 Y_2 &= 1.0e-04 * \begin{bmatrix} -0.1775 & -0.1215 & 0.2785 \\ -0.1215 & -0.1661 & 0.1778 \\ 0.2785 & 0.1778 & -0.6487 \end{bmatrix}, \Gamma_2 = \begin{bmatrix} 0.2432 & -0.0001 & 0.0012 \\ -0.0001 & 0.2438 & 0.0002 \\ 0.0012 & 0.0002 & 0.2441 \end{bmatrix}.
 \end{aligned}$$

We get the following control gain matrices.

$$K_1 = Y\mathbb{P}_1^{-1} = \begin{bmatrix} -0.0429 & -0.0071 & 0.0270 \\ -0.0205 & -0.0062 & 0.0130 \\ 0.0660 & 0.0105 & -0.0446 \end{bmatrix}, K_2 = Y\mathbb{P}_2^{-1} = \begin{bmatrix} -0.0460 & -0.0090 & 0.0305 \\ -0.0311 & -0.0091 & 0.0212 \\ 0.0851 & 0.0166 & -0.0615 \end{bmatrix}.$$



From Figure 7 it reveals that the proposed approaches maximal ranges of sampling period with the minimal number of decision variables. By setting the initial values $\mathbb{V}(\mathfrak{s})$, the state response of system states and control responses of system (18) are presented in Figures 6 and 8 respectively. From Figure 6 we can observe that the system states tends to zero asymptotically. Under the consideration of gain matrices and initial values $\omega(\alpha(\mathfrak{s})) = [-0.1, 0.2, 0.3]^T$, the system states and control responses of the chaotic system [44] are depicted in Figure 8.

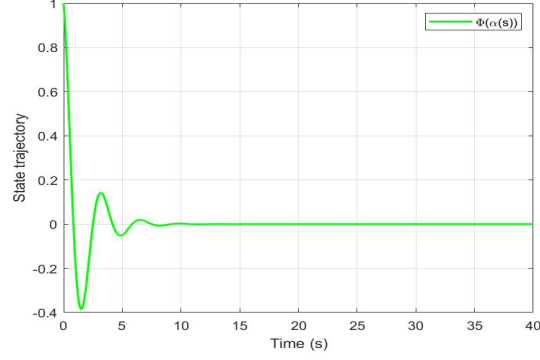
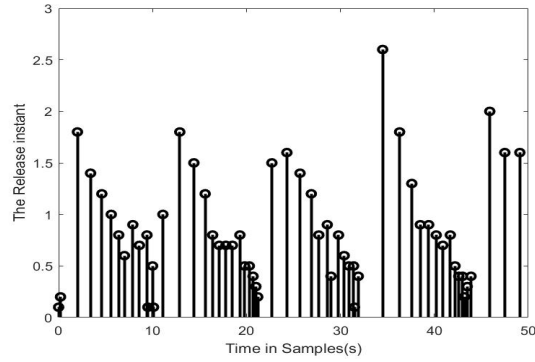
Figure 6: Time responses of system states $\Psi_R(\alpha(\mathfrak{s}))$, $\Psi_g(\alpha(\mathfrak{s}))$, $\Phi(\alpha(\mathfrak{s}))$ and $\eta(\alpha(\mathfrak{s}))$ 

Figure 7: Fuzzy control with event-triggered strategy

6 Conclusions

This study investigated the H_∞ analysis of variable-speed wind turbine systems using an event-triggered method. First, the fuzzy-membership-dependent Lyapunov function is constructed, in which the information about the membership functions will provide effective results on T-S fuzzy-based models. Second, by taking direct wind speed as an external disturbance, the dissipative stability and stability conditions for addressing system (12) with known and unknown gain matrices have been derived in Theorem 4.1 and Theorem 4.2, respectively. Besides, the H_∞ conditions for closed-loop T-S fuzzy systems have been provided in Theorem 4.2 has been derived to ensure the asymptotic stability. After that, the theoretical results of Theorem 4.2 have been affirmed numerically through design examples in numerical validation. Finally, the resulting conditions of Theorem 4.2 have been demonstrated through the existing chaotic Rossler system, ensuring their effectiveness in the comparison example. Simulation examples have been presented to illustrate the effectiveness and the merits of the proposed results. Future work, expand our research to include multi-agent systems, fuzzy-switched systems, switched Boolean networks, fuzzy filtering, and adaptive fuzzy control. Moreover, the determination of partial and time-varying transition probabilities in our framework is an open problem

Methods	$v_m = v_M$	NDVs
38	0.0959	$58n^2 + 6n + 2nm$
39	0.1147	$55n^2 + 4n + 2nm$
40	0.1165	$43.5n^2 + 3.5n + 2nm$
34	0.1210	$24.5n^2 + 6.5n + 2nm$
41	0.2009	$32n^2 + 7n + 2nm$

Table 1: Comparison results of sampling period and computational complexity

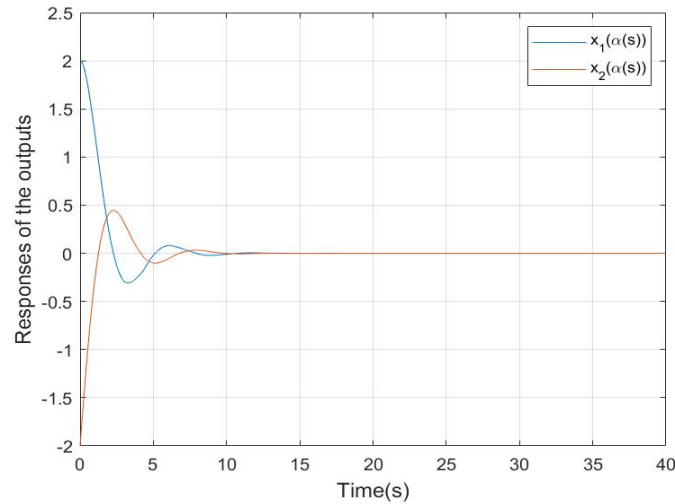


Figure 8: State trajectory of systems (30) is asymptotically stable

to be addressed in the future. Addressing the above imperfections is another issue to be further investigated.

Data availability statement

The authors does not have any conflict of interest.

Acknowledgement

The authors extend their appreciation to the Deanship of Research and Graduate Studies at King Khalid University for funding this work through a Large Research Project under grant number RGP2/55/46.

References

- [1] P. Anbalagan, Y. H. Joo, *Dissipative-based sampled-data control for T-S fuzzy wind turbine system via fragmented-delayed state looped functional approach*, *Nonlinear Dynamics*, **111**(3) (2023), 2463-2486. <https://doi.org/10.1007/s11071-022-07924-3>
- [2] K. A. Banu, T. Aparna, M. M. Tajudeen, G. Rajchakit, T. Huang, *H_∞ control for fractional order neural networks with uncertainties subject to deception attacks via improved memory-event-triggered scheme and its application*, *Neural Networks*, **184** (2025), 107092. <https://doi.org/10.1016/j.neunet.2024.107092>
- [3] R. D. Bianchi, R. J. Mantz, F. Carlos, *Gain scheduling control of variable-speed wind energy conversion systems using quasi-LPV models*, *Control Engineering Practice*, **13**(2) (2005), 247-255. <https://doi.org/10.1016/j.conengprac.2004.03.006>
- [4] G. Brundhashree, S. Shanmugam, S. Magudeeswaran, R. Vadivel, N. Gunasekaran, M. Rhaima, *Master-slave synchronization for fuzzy markovian jump complex dynamical networks with coupling delay via fault-tolerant control*, *International Journal of Fuzzy Systems*, (2024), 1-20. <https://doi.org/10.1007/s40815-024-01880-3>
- [5] W. Cai, Y. Chen, J. Guo, B. Han, Y. Shi, L. Ji, J. Wang, G. Zhang, J. Luo, *Accurate detection of atrial fibrillation from 12-lead ECG using deep neural network*, *Computers in Biology and Medicine*, **116** (2020), 103378. <https://doi.org/10.1016/j.combiomed.2019.103378>
- [6] X. Cai, J. Wang, K. Shi, S. Zhong, T. Jiang, *Quantized dissipative control based on T-S fuzzy model for wind generation systems*, *ISA Transactions*, **126** (2021), 533-544. <https://doi.org/10.1016/j.isatra.2021.08.018>

- [7] J. Cheng, J. H. Park, L. Zhang, Y. Zhu, *An asynchronous operation approach to event-triggered control for fuzzy Markovian jump systems with general switching policies*, IEEE Transactions on Fuzzy Systems, **26**(1) (2018), 6-18. <https://doi.org/10.1109/TFUZZ.2016.2633325>
- [8] R. Datta, R. Saravanakumar, *New insights on dissipative control technique for Takagi-Sugeno fuzzy system with variable time-delays and random packet dropouts*, The European Physical Journal Special Topics, (2024), 1-19. <https://doi.org/10.1140/epjs/s11734-024-01360-7>
- [9] K. Ding, Q. Zhu, *Extended dissipative anti-disturbance control for delayed switched singular semi-Markovian jump systems with multi-disturbance via disturbance observer*, Automatica, **128** (2021), 109556. <https://doi.org/10.1016/j.automatica.2021.109556>
- [10] N. Gunasekaran, M. Manigandan, S. Vinoth, R. Vadivel, *Analysis of caputo sequential fractional differential equations with generalized Riemann-Liouville boundary conditions*, Fractal and Fractional, **8**(8) (2024), 457. <https://doi.org/10.3390/fractalfract8080457>
- [11] S. He, F. Liu, *Finite-time H_∞ fuzzy control of nonlinear jump systems with time delays via dynamic observer-based state feedback*, IEEE Transactions Fuzzy Systems, **20**(4) (2012), 605-614. <https://doi.org/10.1109/TFUZZ.2011.2177842>
- [12] C. Hua, S. Wu, X. Guan, *Stabilization of T-S fuzzy system with time delay under sampled-data control using a new looped-functional*, IEEE Transactions on Fuzzy Systems, **28**(2) (2019), 400-407. <https://doi.org/10.1109/TFUZZ.2019.2906040>
- [13] A. Karnan, G. Soundararajan, G. Nagamani, A. Kashkynbayev, *Design of an event-triggered extended dissipative state estimator for neural networks with multiple time-varying delays*, The European Physical Journal Special Topics, (2024), 1-15. <https://doi.org/10.1140/epjs/s11734-024-01240-0>
- [14] R. Kavikumar, R. Sakthivel, O. M. Kwon, B. Kaviarasan, *Finite-time boundedness of interval type-2 fuzzy systems with time delay and actuator faults*, Journal of the Franklin Institute, **356**(15) (2019), 8296-8324. <https://doi.org/10.1016/j.jfranklin.2019.07.031>
- [15] A. Kazemy, R. Saravanakumar, *Event-triggered networked cascade control systems design subject to hybrid attacks*, Mathematical Methods in the Applied Sciences, **47**(4) (2024), 2609-2622. <https://doi.org/10.1002/mma.9767>
- [16] M. Kchaou, H. Jerbi, *Reliable H_∞ and passive fuzzy observer-based sliding mode control for nonlinear descriptor systems subject to actuator failure*, International Journal of Fuzzy Systems, **24**(1) (2022), 105-120. <https://doi.org/10.1007/s40815-021-01121-x>
- [17] M. Kchaou, M. Syed Ali, B. Vigneshwar, S. Sanober, T. F. Ibrahim, F. D. Alanazi, *Discrete-time uncertain event-triggered H_∞ control for slow sampling Markov jump systems with strictly dissipativity*, Mathematical Methods in the Applied Sciences, **48**(11) (2025), 10896-10908. <https://doi.org/10.1002/mma.10928>
- [18] X. Liu, Z. Gao, M. A. Q. Chen, *Takagi-Sugeno fuzzy model based fault estimation and signal compensation with application to wind turbines*, IEEE Transactions on Industrial Electronics, **64**(7) (2017), 5678-5689. <https://doi.org/10.1109/TIE.2017.2677327>
- [19] Y. Liu, J. H. Park, B. Z. Guo, Y. Shu, *Further results on stabilization of chaotic systems based on fuzzy memory sampled-data control*, IEEE Transactions on Fuzzy Systems, **26**(2) (2017), 1040-1045. <https://doi.org/10.1109/TFUZZ.2017.2686364>
- [20] Q. Lu, P. Shi, L. Wu, H. Zhang, *Event-triggered interval type-2 T-S fuzzy control for nonlinear networked systems*, Journal of the Franklin Institute, **357**(14) (2020), 9834-9852. <https://doi.org/10.1016/j.jfranklin.2020.08.001>
- [21] Z. Lu, X. Zhong, X. Liu, J. Wang, X. Diao, *Energy storage electrochromic devices in the era of intelligent automation*, Physical Chemistry Chemical Physics, **23**(26) (2021), 14126-14145. <https://doi.org/10.1039/D1CP01398J>
- [22] P. Mani, Y. H. Joo, *Fuzzy event-triggered control for back to back converter involved PMSG-based wind turbine systems*, IEEE Transaction on Fuzzy Systems, **30**(5) (2021), 1409-1420. <https://doi.org/10.1109/TFUZZ.2021.3059949>

- [23] P. Mani, Y. H. Joo, *Fuzzy-logic-based event-triggered H_∞ control for networked systems and its application to wind turbine systems*, Information Sciences, **585** (2022), 144-161. <https://doi.org/10.1016/j.ins.2021.11.039>
- [24] S. Mobayen, J. Ma, *Robust finite-time composite nonlinear feedback control for synchronization of uncertain chaotic systems with nonlinearity and time-delay*, Chaos Solitons and Fractal, **114** (2018), 46-54. <https://doi.org/10.1016/j.chaos.2018.06.020>
- [25] J. Mrazgua, R. Chaibi, E. H. Tissir, M. Ouahi, *Static output feedback stabilization of T-S fuzzy active suspension systems*, Journal of Terramechanics, **97** (2021), 19-27. <https://doi.org/10.1016/j.jterra.2021.05.001>
- [26] P. Muthukumar, P. Balasubramaniam, K. T. Ratnavelu, *T-S fuzzy predictive control for fractional order dynamical systems and its applications*, Nonlinear Dynamics, **86**(2) (2016), 751-763. <https://doi.org/10.1007/s11071-016-2919-6>
- [27] G. Panneerselvam, P. Mani, *Event-triggered control for fuzzy-based networked wind-turbines-integrated power systems with distributed communication delays*, IEEE Access, **13** (2025), 35339-35354. <https://doi.org/10.1109/ACCESS.2025.3543720>
- [28] R. Saravanakumar, Y. H. Joo, *Fuzzy dissipative and observer control for wind generator systems a fuzzy time-dependent LKF approach*, Nonlinear Dynamics, **97** (2019), 2189-2199. <https://doi.org/10.1007/s11071-019-05116-0>
- [29] D. Shah, A. Mehta, K. Patel, A. Bartoszewicz, *Event-triggered discrete higher-order SMC for networked control system having network irregularities*, IEEE Transactions on Industrial Informatics, **16**(11) (2019), 6837-6847. <https://doi.org/10.1109/TII.2020.2973739>
- [30] S. Shi, Z. Fei, P. Shi, C. K. Ahn, *Asynchronous filtering for discrete-time switched T-S fuzzy systems*, IEEE Transactions on Fuzzy Systems, **28**(8) (2020), 1531-1541. <https://doi.org/10.1109/TFUZZ.2019.2917667>
- [31] R. Sitharthan, M. Karthikeyan, D. S. Sundar, S. Rajasekaran, *Adaptive hybrid intelligent MPPT controller to approximate effectual wind speed and optimal rotor speed of variable speed wind turbine*, IAS Transactions, **96** (2020), 479-489. <https://doi.org/10.1016/j.isatra.2019.05.029>
- [32] X. Sun, Q. Zhang, *Admissibility analysis for interval type-2 fuzzy descriptor systems based on sliding mode control*, IEEE Transactions on Cybernetics, **49**(8) (2019), 3032-3040. <https://doi.org/10.1109/TCYB.2018.2837890>
- [33] M. Syed Ali, B. Vigneshwar, G. Rajchakit, B. Priya, G. K. Thakur, *Event-triggered H_∞ filtering for TS fuzzy discrete-time conic-type nonlinear networked control systems*, Iranian Journal of Fuzzy Systems, **21**(3) (2024), 137-154. <https://doi.org/10.22111/ijfs.2024.46459.8184>
- [34] N. M. Thoiyab, S. Shanmugam, R. Vadivel, N. Gunasekaran, *Frobenius norm-based global stability analysis of delayed bidirectional associative memory neural networks*, Symmetry, **17**(2) (2025), 183. <https://doi.org/10.3390/sym17020183>
- [35] R. Vadivel, S. Sabarathinam, G. Zhai, N. Gunasekaran, *Event-triggered reachable set estimation for synchronization of Markovian jump complex-valued delayed neural networks under cyber-attacks*, The European Physical Journal Special Topics, (2024), 1-21. <https://doi.org/10.1140/epjs/s11734-024-01372-3>
- [36] B. Vigneshwar, M. Syed Ali, R. Perumal, M. Kchaou, M. Amine Regaieg, H. Jerbi, *H_∞ fault detection and control of Takagi-Sugeno continuous-time conic-type nonlinear systems*, International Journal of Computer Mathematics, **101**(8) (2024), 1-12. <https://doi.org/10.1080/00207160.2024.2353182>
- [37] B. Vigneshwar, M. Syed Ali, R. Perumal, B. Priya, G. K. Thakur, *Event-triggered H_∞ and reduced-order asynchronous filtering for fuzzy Markov jump systems with time-varying delays*, Optimal Control Applications and Methods, **45**(4) (2024), 1872-1888. <https://doi.org/10.1002/oca.3127>
- [38] F. Wang, S. Zhu, K. Liu, M. Chen, Y. Du, *Impedance modeling of wind turbine-variable speed pumped storage combined operation system*, Energy Report, **7**(6) (2021), 470-478. <https://doi.org/10.1016/j.egyrs.2021.08.017>
- [39] Y. Xia, M. Fu, P. Shi, M. Wang, *Robust sliding mode control for uncertain discrete-time systems with time delay*, IET Control Theory Applied, **4**(4) (2010), 613-624. <https://doi.org/10.1049/iet-cta.2009.0068>

- [40] Z. Xu, X. Li, V. Stojanovic, *Exponential stability of nonlinear state-dependent delayed impulsive systems with applications*, Nonlinear Analysis: Hybrid Systems, **42** (2021), 101088. <https://doi.org/10.1016/j.nahs.2021.101088>
- [41] H. Yan, Y. Tian, H. Li, H. Zhang, Z. Li, *Input-output finite-time mean square stabilization of nonlinear semi-Markovian jump systems*, Automatica, **104** (2019), 82-89. <https://doi.org/10.1016/j.automatica.2019.02.024>
- [42] M. Zhang, P. Shi, Z. Liu, H. Su, L. Ma, *Fuzzy model-based asynchronous H_1 filter design of discrete-time Markov jump systems*, Journal of the Franklin Institute, **354**(18) (2017), 8444-8460. <https://doi.org/10.1016/j.jfranklin.2017.09.032>
- [43] M. Zhang, P. Shi, C. Shen, Z. G. Wu, *Static output feedback control of switched nonlinear systems with actuator faults*, IEEE Transactions on Fuzzy Systems, **28**(8) (2019), 1600-1609. <https://doi.org/10.1109/TFUZZ.2019.2917177>
- [44] R. Zhang, D. Zeng, J. H. Park, Y. Liu, S. Zhong, *A new approach to stabilization of chaotic systems with nonfragile fuzzy proportional retarded sampled-data control*, IEEE Transactions on Cybernetics, **49**(9) (2018), 3218-3229. <https://doi.org/10.1109/TCYB.2018.2831782>
- [45] J. Zhang, F. Zhu, H. R. Karimi, F. Wang, *Observer-based sliding mode control for T-S fuzzy descriptor systems with time delay*, IEEE Transactions on Fuzzy Systems, **27**(10) (2019), 2009-2023. <https://doi.org/10.1109/TFUZZ.2019.2893220>
- [46] X. Zhao, W. Xinyong, Z. Guangdeng, H. Li, *Fuzzy-approximation-based adaptive output-feedback control for uncertain non-smooth nonlinear systems*, IEEE Transactions on Fuzzy Systems, **26**(6) (2018), 3847-3859. <https://doi.org/10.1109/TFUZZ.2018.2851208>
- [47] Q. Zhu, *Stabilization of stochastic nonlinear delay systems with exogenous disturbances and the event-triggered feedback control*, IEEE Transactions on Automatic Control, **64**(9) (2018), 3764-3771. <https://doi.org/10.1109/TAC.2018.2882067>